The British Journal of Radiology, 85 (2012), 153–160

Estimation of paediatric organ and effective doses from dental cone beam CT using anthropomorphic phantoms

[1,2]C THEODORAKOU, BSc, MSc, PhD, [2]A WALKER, BSc, MSc, FIPEM, [1]K HORNER, BCHD, PhD, FRCR, [3]R PAUWELS, BSc, MSc, [4]R BOGAERTS, BSc, MSc, PhD, [3]R JACOBS DDS, MSc, PhD and [5]THE SEDENTEXCT PROJECT CONSORTIUM

[1]*North Western Medical Physics, The Christie NHS Foundation Trust and* [2]*School of Dentistry, University of Manchester, Manchester Academic Health Science Centre, Manchester, UK,* [3]*Oral Imaging Centre, School of Dentistry, Oral Pathology and Maxillofacial Surgery, Faculty of Medicine and* [4]*Department of Experimental Radiotherapy, University Hospital Gasthuisberg, Katholieke Universiteit Leuven, Belgium, and* [5]*www.sedentexct.eu (list of partners)*

Objectives: Cone beam CT (CBCT) is an emerging X-ray technology applied in dentomaxillofacial imaging. Previous published studies have estimated the effective dose and radiation risks using adult anthropomorphic phantoms for a wide range of CBCT units and imaging protocols.
Methods: Measurements were made five dental CBCT units for a range of imaging protocols, using 10-year-old and adolescent phantoms and thermoluminescent dosimeters. The purpose of the study was to estimate paediatric organ and effective doses from dental CBCT.
Results: The average effective doses to the 10-year-old and adolescent phantoms were 116 μSv and 79 μSv, respectively, which are similar to adult doses. The salivary glands received the highest organ dose and there was a fourfold increase in the thyroid dose of the 10-year-old relative to that of the adolescent because of its smaller size. The remainder tissues and salivary and thyroid glands contributed most significantly to the effective dose for a 10-year-old, whereas for an adolescent the remainder tissues and the salivary glands contributed the most significantly. It was found that the percentage attributable lifetime mortality risks were 0.002% and 0.001% for a 10-year-old and an adolescent patient, respectively, which are considerably higher than the risk to an adult having received the same doses.
Conclusion: It is therefore imperative that dental CBCT examinations on children should be fully justified over conventional X-ray imaging and that dose optimisation by field of view collimation is particularly important in young children.

Received 29 March 2010
Revised 3 November 2010
Accepted 9 November 2010

DOI: 10.1259/bjr/19389412

Cone beam CT (CBCT) is an advancement of CT technology that has found wide application in dentomaxillofacial imaging. The ability of the CBCT systems to produce three-dimensional high-resolution images with diagnostic reliability has resulted in a significant increase in CBCT examinations in areas such as orthodontics, endodontics, periodontics, implantology, restorative dentistry, and dental and maxillofacial surgery [1–12]. However, CBCT imaging is associated with a higher radiation dose to the patient than panoramic and intra-oral imaging but a lower patient dose than conventional single and multislice CT [13–16]. Although radiation dose from CBCT is low relative to conventional CT, the radiation risk to the patient should be assessed and quantified. The radiation risk can be estimated by calculating the effective dose, which is a radiation quantity proposed by the International Commission on Radiological Protection (ICRP) [17].

Several studies have estimated the effective dose for a range of CBCT units and imaging protocols [13–16, 18–24]. The organ doses were measured with anthropomorphic phantoms and thermoluminescent dosimeters (TLDs). The ICRP 103 [25] tissue weighting factors were applied to organ doses to account for the tissue radiosensitivity. The ICRP 60 [17] and the revised ICRP 103 [25] tissue weighting factors have been used for studies before and after 2006, respectively. For the head and neck region, the ICRP 103 [25] factors include the salivary glands, oral mucosa and lymph nodes as radiosensitive organs that were not included in ICRP 60 [17]. In addition, the weighting factor of the remainder tissues was increased from 0.05 to 0.12. The published effective doses range from a few tens to several hundreds of microsieverts

Address correspondence to: Dr Chrysoula Theodorakou, North Western Medical Physics, The Christie NHS Foundation Trust, Wilmslow Road, Manchester, M20 4BX, UK. E-mail: christie.theodorakou@physics.cr.man.ac.uk
The research leading to these results has received funding from the European Atomic Energy Community's Seventh Framework Programme FP7/2007–2011 under grant agreement no 212246 (SEDENTEXCT: Safety and Efficacy of a New and Emerging Dental X-ray Modality).

depending on the CBCT unit, the field of view and the position of the radiation field with respect to the radiosensitive organs.

To the best knowledge of the authors, all the published studies on dental CBCT dosimetry have focused on effective doses to adult patients for a range of CBCT units and imaging protocols but none has estimated the organ and effective doses to paediatric patients. Children are more sensitive to radiation than adults because the number of dividing cells promoting DNA mutagenesis is higher and they have more time to express any radiation-induced effects, such as cancer. There is an order of magnitude increase in cancer risk between children and adults, and there is also a significant difference between boys and girls, with the latter being more radiosensitive [26, 27]. Furthermore, a substantial proportion of dental X-ray procedures are performed in the paediatric group, notably in relation to orthodontics.

The aim of this study was to measure paediatric organ doses and, hence, derive effective doses using two anthropomorphic phantoms and TLDs for a range of CBCT units and for standard imaging protocols.

Methods and materials

Anthropomorphic phantoms

Two tissue-equivalent anthropomorphic phantoms (ATOM Model 702-C and ATOM Model 706-C; Computerized Imaging Reference Systems Inc, Norfolk, VA) were used. Models 706-C and 702-C simulate a 10-year-old child and an adult female, respectively. An adult female phantom was used to simulate an adolescent patient as there are no commercially available adolescent anthropomorphic phantoms. The ICRP 89 [28] reference values for body height for a 15-year-old male and female are 167 cm and 161 cm, respectively, compared with 160 cm for the female ATOM phantom. The weight of the female ATOM phantom is 55 kg compared with the ICRP 89 [28] reference weight values of 56 kg and 53 kg for a 15-year-old male and female, respectively. The ATOM phantom design was based on ICRP 23 [29] and ICRU 48 [30] and available anatomical reference data. The tissues simulated in the ATOM phantoms are average bone, soft tissue, cartilage, spinal cord, spinal disks, lung, brain, sinus, trachea and bronchial cavities. The density of the simulated paediatric bone is typical of the phantom's age. The bone tissue is an average of known cortical-to-trabecular ratios and age-based mineral densities.

The ATOM phantoms are available in 25 mm slices and for the purposes of this study the head, neck and shoulders of both phantoms were used. Figures 1a and b show the ATOM 702-C (female) and 706-C (10-year-old) phantoms, respectively.

Thermoluminescent dosimeters

All dose measurements were performed using TLD chips: TLD-100H, LiF:Mg,Cu,P (Harshaw Thermo Fisher Scientific Inc, Waltham, MA). The TLDs were calibrated free in air against a 6-cm^3 ionisation chamber (Radcal 9010; Radcal Corporation, Monrovia, CA) coupled with an electrometer (Radcal 9010, Radcal Corporation) with calibration traceable to national standards (National Physical Laboratory) using a conventional diagnostic X-ray tube at 80 kV (half-value layer=3.02 mm Al). The energy response was within the TLD statistical error (<5%) for a tube voltage range of 60 kV to 100 kV. Chips with a reproducibility error of <10% were used. The chips were read using an automatic TLD reader (Harshaw 5500; Harshaw Thermo Fisher Scientific Inc). Five TLDs were used for measuring the background signal.

(a) (b)

Figure 1. (a) ATOM Model 702-C. (b) ATOM Model 706-C.

Organ and effective dose estimation

The salivary and thyroid glands, brain, red bone marrow, bone surface, oral mucosa, oesophagus, extrathoracic airway, lymph nodes, muscle and lungs are the radiosensitive organs located in the head, neck and upper chest region according to ICRP 103 [25]. Initially, the dose to the lungs was measured but it was found that the contribution to the effective dose was insignificant (<1%). Therefore, for organs located outside the region of the head, neck and upper chest it was assumed that the dose was zero. The bone surface dose was assumed to be equal to the red bone marrow dose. The dose to the oesophagus was assumed to be equal to the thyroid gland dose, but after the fractionation to account for the partial irradiation of the organ, it was found that the contribution to the effective dose was less than 1% and therefore was not taken into account for the effective dose calculations. The tissue weighting factor w_T for the remainder tissues was increased from 0.05 in ICRP 60 [17] to 0.12 in ICRP 103 [25]. Therefore, the contribution of the remainder tissues to the effective dose in dental CBCT cannot be neglected. In the head and neck region, the remainder tissues are the oral mucosa, extrathoracic airway, lymph nodes and muscle. Similar to Ludlow and colleagues [15, 19], Roberts et al [14], Suomalainen et al [18] and ICRP 66 [31], it was assumed that the dose to the oral mucosa equals the dose to the salivary glands; the dose to the lymph nodes and muscle equals the average dose to the thyroid gland, submandibular and parotid glands; and the dose to the extrathoracic airway equals the average dose to the thyroid gland, salivary glands, and bone marrow located at the anterior nasal cavity.

For the brain, salivary glands, thyroid gland, extrathoracic airway and oral mucosa, TLDs were positioned uniformly throughout the organ volume and therefore the factors f_i that account for the fraction of the total mass of the specified organ in the phantom slice i were reduced to unity. For skin, bone and red bone marrow, the average doses per slice were fractionated using the f_i values from the Huda and Sandison [32] study. For the remainder tissues, it was assumed that 5% of the lymph nodes and muscle are located in the head and neck region [14]. The dose to the remainder tissues was calculated as the arithmetic mean over the 13 remainder organs [25]. The effective dose was calculated as the product of the radiation weighted average organ doses and the relevant ICRP 103 [25] tissue weighting factors summed over all of the tissues/organs exposed.

Table 1 shows the number of TLDs per organ and the slices where the TLDs were positioned.

CBCT units and imaging protocols

Table 2 shows the CBCT units used in this study with manufacturer details and Tables 3 and 4 summarise the imaging protocols and exposure factors, respectively. The most frequently used imaging protocols on each system were selected. Thus, in the 10-year-old phantom, maxillary anterior examinations were included, reflecting the use of imaging in orthodontic examinations of tooth eruption abnormalities in this aesthetically important part of the mouth. By contrast, for the adolescent phantom, third molar examinations were included to reflect the increasing clinical need for imaging of this area. Both phantoms were positioned as patients with the aid of radiographers and the machines' alignment tools, such as lasers and scout images. Since a scout image is part of the clinical protocol for setting up the patient, one scout image was included in each measurement. Thyroid collars were not used for the phantoms because it is not a common practice among the different dental hospitals and dental practices to routinely use such devices.

All of the CBCT units shown in Table 4, with the exception of 3D Accuitomo 170, adjust the mAs automatically and the tube voltage is either fixed (NewTom VG and i-CAT NG) or manually selected. For the units for which the exposure settings were not selected automatically, the exposures were made at the recommended manufacturers' settings. At the time of the measurements, the units did not provide specialised paediatric protocols and settings. The ProMax 3D and Kodak 9000C 3D units provided settings for different patient sizes. For the Promax 3D, the small size was selected for both phantoms, but the mAs was adjusted automatically based on the phantom size. For the Kodak 9000C 3D, the ''teenager'' setting was chosen for the 10-year-old phantom and the ''adult'' setting for the adolescent, to provide adequate image quality. For the 3D Accuitomo 170, the manufacturer's settings of 90 kV, 5 mA, 17.5 s, which corresponds to a 360° rotation, were selected for all fields of view.

Table 1. Location and number of thermoluminescent dosimeters (TLDs) in the two ATOM phantoms (refer to Figure 1)

Organ	Adolescent phantom		10-year-old phantom	
	Number of TLDs	Slices	Number of TLDs	Slices
Brain	35	2–6	27	2–7
Right submandibular gland	2	8	2	7
Left submandibular gland	2	8	2	7
Right parotid gland	3	6–7	2	6
Left parotid gland	3	6–7	2	6
Sublingual gland	2	8	2	7
Thyroid gland	7	10–11	7	9–10
Red bone marrow	58	2–12	36	2–11
Skin	24	2–12	22	2–11
Anterior nasal passage	4	5–6	2	6

Table 2. Dental cone beam CT units

Model	Manufacturer
NewTom VG	QR SRL, Verona, Italy
Next Generation i-CAT (i-CAT NG)	Imaging Sciences International, Hatfield, PA
3D Accuitomo 170	J. Morita MFG. Corp., Kyoto, Japan
ProMax 3D	Planmeca Oy, Helsinki, Finland
Kodak 9000C 3D	Kodak Dental Systems by Carestream Health, Rochester, MJ

Table 3. Imaging protocols and fields of view

	Adolescent phantom	10-year-old phantom	Field of view
i-CAT NG			Ø16 cm and
	(i) Mandible	(i) Mandible	(i) 6 cm height
	(ii) Maxilla	(ii) Maxilla	(ii) 6 cm height
	(iii) Maxillofacial	(iii) Maxillofacial	(iii) 13 cm height
NewTom VG	Dental	Dental	Ø15 × 11 cm height
Kodak 9000C 3D	Third molar	Maxillary anterior	Ø5 × 3.7 cm height
ProMax 3D	Dentoalveolar	Dentoalveolar	Ø8 × 8 cm height
3D Accuitomo 170	(i) Third molar	(i) Maxillary anterior	(i) 4 × 4 cm height
	(ii) Maxilla	(ii) Mandible	(ii) Ø14 cm × 5 cm height
	(iii) Dentoalveolar	(iii) Dentoalveolar	(iii) Ø14 × 10 cm height
	(iv) Maxillofacial	(iv) Maxillofacial	(iv) Ø17 × 12 cm height

Results

Figure 2 and Figure 3 show the effective doses calculated for the 10-year-old and adolescent phantoms respectively for the five CBCT units and for all the imaging protocols.

The average effective doses for the 10-year-old and adolescent phantoms were 116 μSv and 79 μSv, respectively. The minimum effective dose for the 10-year-old phantom was 16 μSv and for the adolescent was 18 μSv, whereas the maximum effective doses for the 10 year old and the adolescent were 282 μSv and 216 μSv, respectively. For the 10-year-old phantom and for the large fields of view such as the 17×12 cm^2 and 14×10 cm^2 of the 3D Accuitomo 170, the single field of view of the NewTom VG and the 13 cm of the i-CAT NG, the effective dose varied between 114 μSv and 282 μSv. Similarly for the adolescent phantom, the effective dose ranged from 81 μSv to 216 μSv. For the small fields of view and for both phantoms, the effective dose did not exceed 35 μSv. For comparison, the effective doses to an adult patient for a typical panoramic examination and a head CT are 10 μSv and 2 mSv, respectively [33].

Figure 4 shows the average organ doses for both phantoms. The organ doses for the 10-year-old phantom were higher than the adolescent, with the salivary glands receiving higher doses than the rest of the organs for both phantoms. Figure 5 shows the percentage contribution of each organ dose to the effective dose for both phantoms.

Discussion

The effective dose for the 10 year old was higher than the effective dose for the adolescent for most of the CBCT units and imaging protocols. For the Kodak 9000C 3D, the effective doses were almost the same for the two phantoms, and for the 4×4 cm^2 field of view of the 3D Accuitomo 170, the effective dose of the adolescent phantom was higher because the imaging protocols for the two phantoms were different, with the radiation field of the adolescent's imaging protocol being closer to the salivary glands. The lowest effective doses were given by the Kodak 9000C 3D and the ProMax 3D owing to the small fields of view, low exposure factors and position of the radiation field with respect to the radiosensitive organs. For both phantoms, the maximum effective doses were calculated for the maxillofacial imaging protocols (large fields of view) of the 3D Accuitomo 170. The 3D Accuitomo 170 effective doses for the maxillofacial imaging protocols were considerably higher than the i-CAT NG and the NewTom VG maxillofacial imaging protocols, and this is due to the higher mAs used by the 3D Accuitomo 170. It should be noted that the standard manufacturer's exposure settings were used for the 3D Accuitomo exposures, while for the i-CAT NG and the NewTom VG the exposure factors were automatically selected by the CBCT unit. The i-CAT NG-13 cm portrait and the NewTom VG-Dental exposed both phantoms to lower doses than the maxillofacial protocols of the 3D Accuitomo 170.

Table 4. Exposure factors

	Adolescent phantom			10-year-old phantom		
	kV	mAs	Voxel size (mm^3)	kV	mAs	Voxel size (mm^3)
i-CAT NG	120	18.5	0.4	120	18.5	0.4
NewTom VG	110	Auto	0.3	110	Auto	0.3
Kodak 9000C 3D	70	106.8	0.076	70	85.6	0.076
ProMax 3D	84	19.6	0.32	84	16.8	0.32
3D Accuitomo 170	90	87.5	0.08–0.25	90	87.5	0.08–0.25

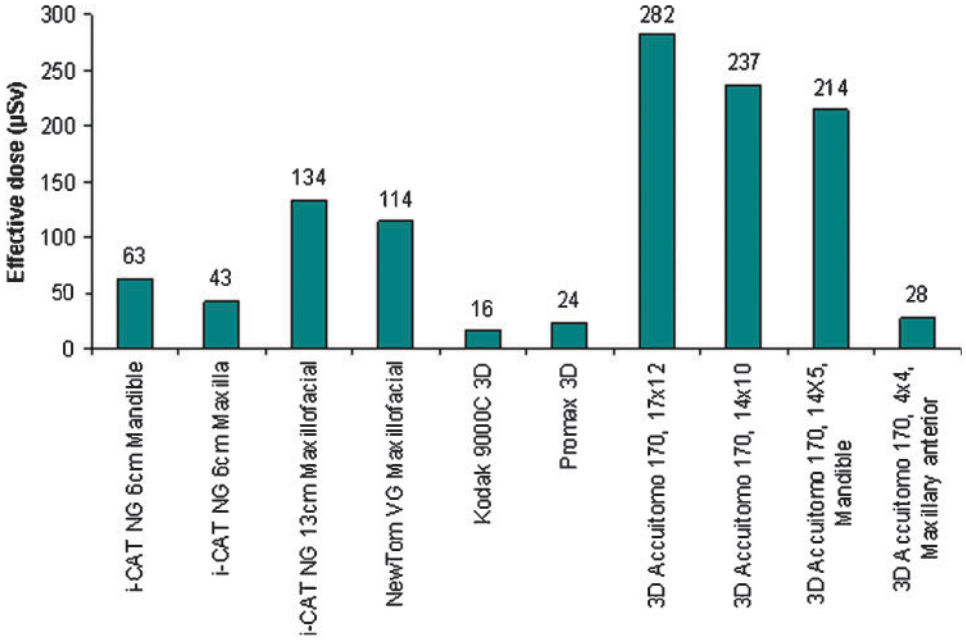

Figure 2. Effective dose (μGy) for a 10 year old (ATOM model 706-C).

The importance of the field of view in the relative difference in effective dose between the adolescent and 10-year-old is well illustrated in this study. If the Kodak 9000C 3D, the 4×4 cm^2 3D Accuitomo 170 and the ProMax 3D are considered to be ''small'' fields of view in CBCT examinations, it can be seen that the difference in effective dose between the two phantoms was small. By contrast, for all other CBCT examinations with large fields of view, the effective dose was considerably higher for the 10-year-old. This clearly underlines the importance of limiting field of view as a basic principle [34, 35] of CBCT use but also indicates the even greater significance of this optimisation in younger children.

The organ doses of the 10-year-old phantom were higher than those of the adolescent phantom owing to the smaller size of the 10-year-old phantom. The smaller diameter and height of the 10-year-old phantom's head places the thyroid gland closer to the primary beam, resulting in a fourfold difference between the two thyroid doses, as shown in Figure 4. The rest of the organs are placed closer to the surface; therefore, they are exposed to a less attenuated X-ray beam and higher organ and effective doses. This can be shown by comparing the effective doses between the two phantoms for the large field of view of the 3D Accuitomo 170. Even though the exposure factors and the imaging protocols were the same for both phantoms, the 10-year-old effective dose was 30% higher than the adolescent dose.

For both phantoms, the doses to the salivary glands were significantly higher than the doses to the other organs because they were either partially or fully irradiated by the primary X-ray beam. The doses to the red bone marrow, bone surface, remainder tissues and skin were small. The dose to the brain was relatively

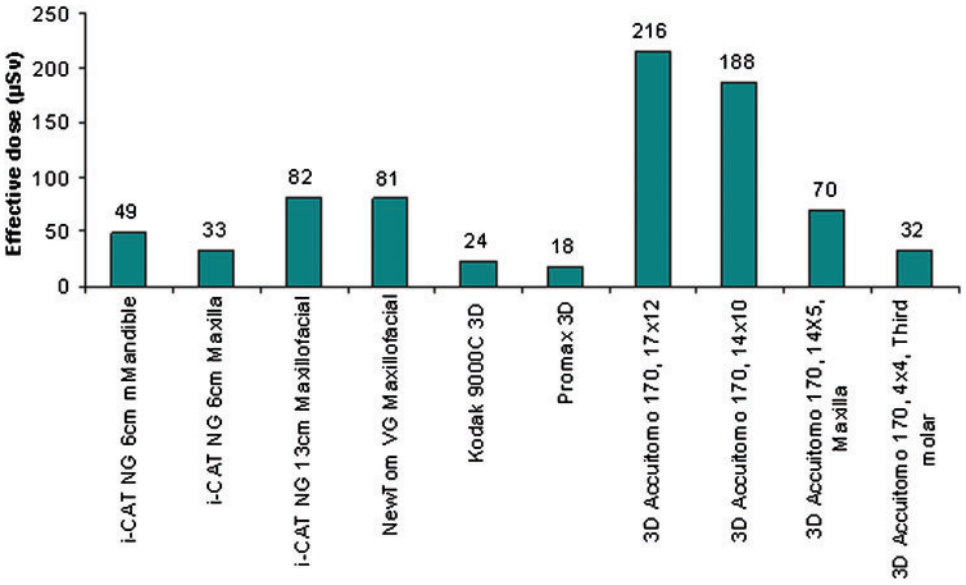

Figure 3. Effective dose (μGy) an adolescent (ATOM model 702-C).

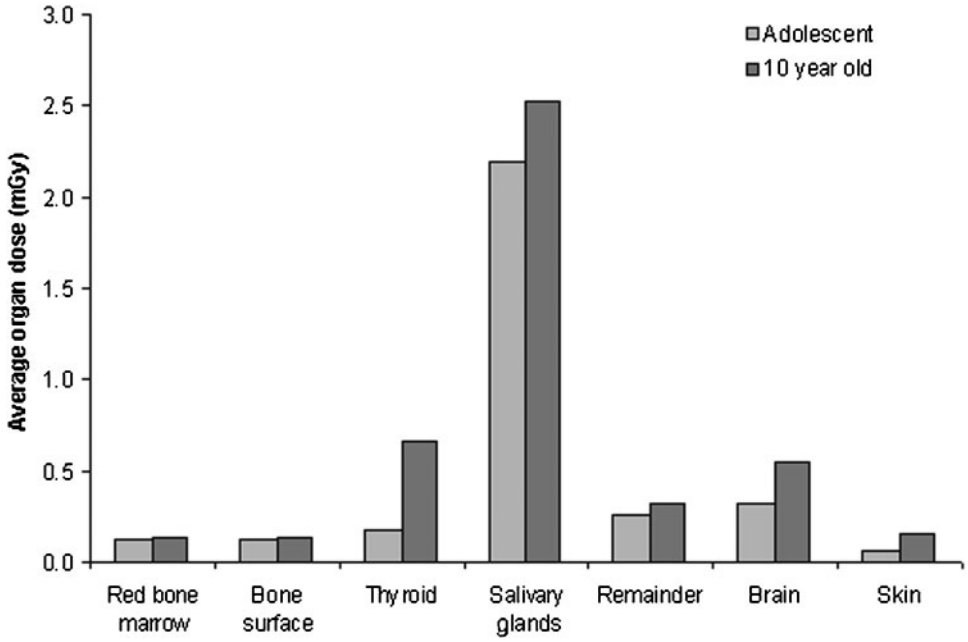

Figure 4. Average organ doses for an adolescent and a 10-year-old patient.

small because this organ was either irradiated by scattered radiation or partially irradiated by the primary beam for the maxillary and maxillofacial imaging protocols.

In ICRP 60 [17], the remainder tissues were assigned a tissue weighting factor of 0.05 and, with the exception of muscle and brain, all of the remainder tissues were located outside the head and neck region. In ICRP 103 [25], the radiosensitivity of the remainder tissues was increased from 0.05 to 0.12 and the list of remainder tissues updated. The brain was assigned an individual weighting factor of 0.01 and removed from the list. Of particular relevance to dental CBCT, the oral mucosa and lymph nodes were added. The doses to the oral mucosa and extrathoracic airway were measured using TLDs that were positioned across the whole volume of the two organs. The lymph nodes and muscles are distributed across the whole body, but TLDs were positioned only in the head and neck area. Therefore, factors [14] were applied to the measured doses for lymph nodes and muscle to account for this. Figure 4 shows that the dose to the remainder tissues was similar to the doses to the red bone marrow, skin and brain but, owing to their high radiosensitivity, the contribution of the remainder tissues to the effective dose was significant, as shown in Figure 5.

For the 10-year-old phantom, the salivary glands, remainder tissues and thyroid glands contributed equally to the effective dose, while for the adolescent phantom the salivary glands and the remainder tissues gave the most significant contribution. Even though the red bone marrow dose was relatively small (Figure 4), its

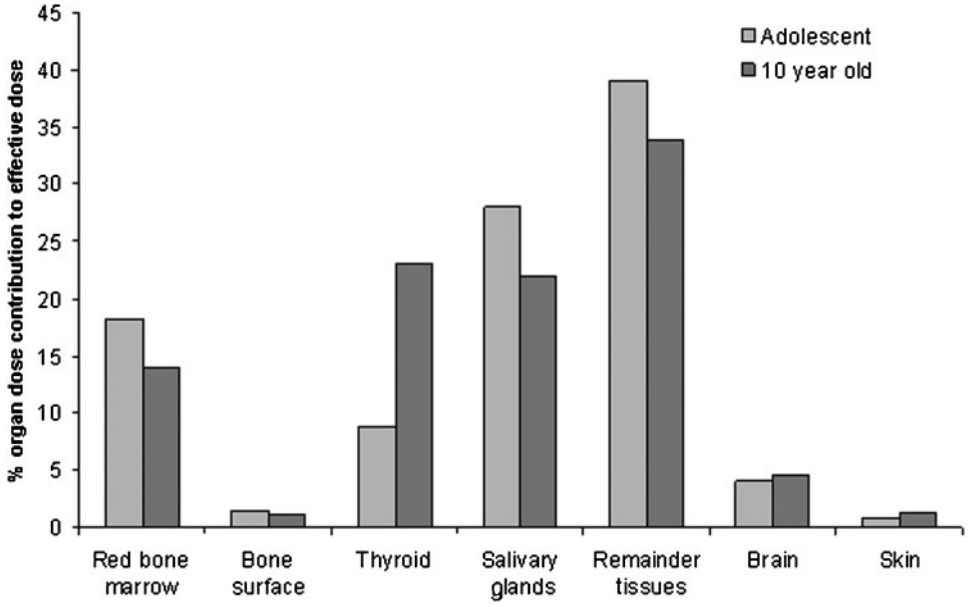

Figure 5. Percentage organ dose contribution to effective dose.

Table 5. Comparison of effective doses of this study with various published studies

Reference	CBCT unit	Effective dose (μSv)
Loubele et al [16]	i-CAT, Accuitomo 3D and NewTom 3G	13–82
Roberts et al [14]	i-CAT	58.9–206.2
Silva et al [22]	NewTom 9000, i-CAT	56.2 and 61.1
Ludlow and Ivanovic [15]	NewTom 3G, CB Mercuray, NG i-CAT, i-CAT, Iluma, Galileos, ProMax 3D PreXion 3D	68–1,073
Hirsch et al [20]	3D Accuitomo, Veraviewepocs 3D	20.02–43.27
Suomalainen et al [18]	3D Accuitomo, ProMax 3D, Scanora 3D	27–674
This study	3D Accuitomo, NewTom VG, ProMax 3D, Kodak 9000C 3D, NG i-CAT	16–282

contribution to the effective dose was significant for both phantoms because of its high radiosensitivity. The contributions of the skin, brain and bone surface were small for both phantoms.

A direct comparison with other studies on paediatric dental CBCT dosimetry was not possible because there are no published paediatric studies using dental CBCT units. All of the published studies on dental CBCT dosimetry investigated organ and effective doses using adult anthropomorphic phantoms. Table 5 compares the effective doses determined in this study with various published studies. It can be seen from Table 5 that this study's effective doses are similar to the effective doses estimated using adult phantoms.

The linear no-threshold (LNT) model of radiation-induced carcinogenesis is the basis for radiation protection considerations at low doses. The LNT model suggests that the relationship between dose and risk is linear and there is no threshold below which the risk becomes zero. The resulting risk factors are primarily based on the life span study (LSS) of atomic bomb survivors [36, 37]. The risk decreases linearly with no threshold for doses below 100 mSv [26, 28, 38]. For very low doses <5 mSv, the National Council on Radiation Protection and Measurements Report [39] supports the linear dose–response relation based on laboratory and epidemiological studies. There are other models that support curvilinear relationships between dose and risk, but given the current knowledge, ICRP 103 [25] risk estimation is based on a linear no-threshold dose–response at low doses.

Another conclusion from the LSS is that children are more sensitive to radiation than adults [26, 27]. There is an order-of-magnitude increase in the attributable lifetime mortality risk between children and adults and there is also a twofold increase in sensitivity between girls and boys. Children have a longer life span to express any radiation-induced cancer and also they are inherently more radiosensitive because they have more dividing cells [26, 27]. The sex-averaged percentage attributable lifetime mortality risk for a child at the age of 10 years was 1.5×10^{-4} and at the age of 15 years was 1.125×10^{-4} [26]. This study estimated that the average effective doses to a 10-year-old and 15-year-old were 116 μSv and 79 μSv, respectively. Based on these figures, the percentage attributable lifetime mortality risk for a 10-year-old and a 15-year-old were 0.00174% and 0.00089%, respectively. For comparative purposes, the percentage attributable lifetime mortality risks for a 50-year-old adult having received an effective dose of 116 μSv and 79 μSv were 0.00075% and 0.00051%.

Conclusions

This study investigated the organ and effective doses for paediatric dental CBCT using anthropomorphic phantoms. Even though the paediatric effective doses were considerably lower than they were for head and neck multislice CT, it was found that they were higher than those for conventional dental X-ray imaging and similar to those for adult CBCT doses. This study has shown that the lowest effective doses were calculated for units that offered small fields of view and ''small patient size'' settings. Therefore, dose reduction can be achieved by using the paediatric or small patient size settings. Small and medium fields of view should be used for mandible and/or maxilla imaging, while for CBCT units which offer only large fields of view, vertical and horizontal collimation should be offered. Taking into account the higher radiosensitivity of children, it is imperative that the use of CBCT in children is fully justified over conventional X-ray imaging.

Further *in vivo* dosimetry studies should be performed to investigate the dose levels for typical paediatric imaging protocols and for a greater range of dental CBCT. The use of entrance surface dose or dose–area product as a diagnostic reference level quantity should be assessed on groups of paediatric patients. Further studies should be undertaken in order to assess the use of a thyroid collar as a dose reduction technique, especially for small paediatric patients.

Acknowledgments

We are grateful to Angela Carson (Dental Hospital, Central Manchester University Hospital NHS Foundation Trust), Jonathan Davies, Nadine White, Ben Johnson and Jackie Brown (Dental Hospital, Guy's and St Thomas' Foundation Trust), Andrew Dawood and Veronique Sauret-Jackson (Cavendish Imaging), Lynda Sheard and Fiona Carmichael (Leeds Dental Institute) and Paul Charnock (Integrated Radiological Services for the Alder Hey Children's Hospital) for giving us access to their dental CBCT units and for assisting us with the measurements. Acknowledgment is given to the support received from the Manchester NIHR Biomedical Research Centre.

References

1. Mah J, Enciso R, Jorgensen M. Management of impacted cuspids using 3-D volumetric imaging. J Calif Dent Assoc 2003;31:935–41.

2. Kau CH, Richmond S, Palomo JM, Hans MG. Three-dimensional cone beam computerized tomography in orthodontics. J Orthod 2005;32:282–93.
3. Wörtche R, Hassfeld S, Lux CJ, Müssig E, Hensley FW, Krempien R, et al. Clinical application of cone beam digital volume tomography in children with cleft lip and palate. Dentomaxillofac Radiol 2006;35:88–94.
4. Cotton TP, Geisler TM, Holden DT, Schwartz SA, Schindler WG. Endodontic applications of cone-beam volumetric tomography. J Endod 2007;33:1121–32.
5. Guerrero ME, Jacobs R, Loubele M, Schutyser F, Suetens P, van Steenberghe D. State-of-the-art on cone beam CT imaging for preoperative planning of implant placement. Clin Oral Investig 2006;10:1–7.
6. Ziegler CM, Woertche R, Brief J, Hassfeld S. Clinical indications for digital volume tomography in oral and maxillofacial surgery. Dentomaxillofac Radiol 2002;31:126–30.
7. Patel S, Dawood A, Ford TP, Whaites E. The potential applications of cone beam computed tomography in the management of endodontic problems. Int Endod J 2007;40:818–30.
8. Kasaj A, Willershausen B. Digital volume tomography for diagnostics in periodontology. Int J Comput Dent 2007; 10:155–68.
9. Nakagawa Y, Kobayashi K, Ishii H, Mishima A, Ishii H, Asada K, et al. Preoperative application of limited cone beam computerized tomography as an assessment tool before minor oral surgery. Int J Oral Maxillofac Surg 2002;31:322–6.
10. Drage NA, Sivarajasingam V. The use of cone beam computed tomography in the management of isolated orbital floor fractures. Br J Oral Maxillofac Surg 2009;47:65–6.
11. Boeddinghaus R, Whyte A. Current concepts in maxillofacial imaging. Eur J Radiol 2008;66:396–418.
12. Hussain AM, Packota G, Major PW, Flores-Mir C. Role of different imaging modalities in assessment of temporomandibular joint erosions and osteophytes: a systematic review. Dentomaxillofac Radiol 2008;37:63–71.
13. Cohnen M, Kemper J, Möbes O, Pawelzik J, Mödder U. Radiation dose in dental radiology. Eur Radiol 2002;12:634–7.
14. Roberts JA, Drage NA, Davies J, Thomas DW. Effective dose from cone beam CT examinations in dentistry. Br J Radiol 2009;82:35–40.
15. Ludlow JB, Ivanovic M. Comparative dosimetry of dental CBCT devices and 64-slice CT for oral and maxillofacial radiology. Oral Surg Oral Med Oral Pathol Oral Radiol Endod 2008;106:106–14.
16. Loubele M, Bogaerts R, Van Dijck E, Pauwels R, Vanheusden S, Suetens P, et al. Comparison between effective radiation dose of CBCT and MSCT scanners for dentomaxillofacial applications. Eur J Radiol 2009;71:461–8.
17. International Commission on Radiological Protection. 1990 Recommendations of the International Commission on Radiological Protection. ICRP Publication 60. Annals of the ICRP. Oxford, UK: Pergamon Press, 1991.
18. Suomalainen A, Kiljunen T, Käser Y, Peltola J, Kortesniemi M. Dosimetry and image quality of four dental cone beam computed tomography scanners compared with multislice computed tomography scanners. Dentomaxillofac Radiol 2009;38:367–78.
19. Ludlow JB, Davies-Ludlow LE, Brooks SL, Howerton WB. Dosimetry of 3 CBCT devices for oral and maxillofacial radiology: CB Mercuray, NewTom 3G and i-CAT NG. Dentomaxillofac Radiol 2006;35:219–26.
20. Hirsch E, Wolf U, Heinicke F, Silva MA. Dosimetry of the cone beam computed tomography Veraviewepocs 3D compared with the 3D Accuitomo in different fields of view. Dentomaxillofac Radiol 2008;37:268–73.
21. Okano T, Harata Y, Sugihara Y, Sakaino R, Tsuchida R, Iwai K, et al. Absorbed and effective doses from cone beam volumetric imaging for implant planning. Dentomaxillofac Radiol 2009;38:79–85.
22. Silva MA, Wolf U, Heinicke F, Bumann A, Visser H, Hirsch E. Cone-beam computed tomography for routine orthodontic treatment planning: a radiation dose evaluation. Am J Orthod Dentofacial Orthop 2008;133:640.e1–5.
23. Tsiklakis K, Donta C, Gavala S, Karayianni K, Kamenopoulou V, Hourdakis CJ. Dose reduction in maxillofacial imaging using low dose cone beam CT. Eur J Radiol 2005;56:413–17.
24. Mah JK, Danforth RA, Bumann A, Hatcher D. Radiation absorbed in maxillofacial imaging with a new dental computed tomography device. Oral Surg Oral Med Oral Pathol Oral Radiol Endod 2003;96:508–13.
25. International Commission on Radiological Protection. Recommendations of the International Commission on Radiological Protection. ICRP Publication 103. Annals of the ICRP 37. Oxford, UK: Pergamon Press, 2007.
26. Brenner DJ. Estimating cancer risks from pediatric CT: going from the qualitative to the quantitative. Pediatr Radiol 2002;32:228–3.
27. Pierce DA, Preston DL. Radiation-related cancer risks at low doses among atomic bomb survivors. Radiat Res 2000;154: 178–86.
28. International Commission on Radiological Protection. Basic anatomical and physiological data for use in radiological protection: reference values. ICRP Publication 89. Oxford, UK: Pergamon Press, 2003.
29. International Commission on Radiological Protection. Reference manual: Anatomical, physiological and metabolic characteristics. ICRP Publication 23. Oxford, UK: Pergamon Press, 1975.
30. International Commission on Radiation Units and Measurements. Phantoms and computational models in therapy, diagnosis and protection. ICRU Report 48. Bethesda, MD: International Commission on Radiation Units and Measurements 1992.
31. International Commission on Radiological Protection. Human respiratory tract model for radiological protection. ICRP Publication 66. Ann ICRP. Oxford, UK: Pergamon Press, 1994.
32. Huda W, Sandison GA. Estimation of mean organ doses in diagnostic radiology from Rando phantom measurements. Health Phys 1984;47:463–7.
33. National Radiological Protection Board. Radiation exposure of the UK population from medical and dental X-ray examinations. Report NRPB-W4. Didcot, UK: Health Protection Agency, 2002.
34. Horner K, Islam M, Flygare L, Tsiklakis K, Whaites E. Basic principles for use of dental cone beam computed tomography: consensus guidelines of the European Academy of Dental and Maxillofacial Radiology. Dentomaxillofac Radiol 2009;38:187–95.
35. The SEDENTEXCT Consortium. Provisional guidelines on CBCT for dental and maxillofacial radiology. [accessed 29 March 2010] Available from: http://www.sedentexct.eu/content/provisional-guidelines-cbct-dental-and-maxillofacial-radiology.
36. Preston DL, Shimizu Y, Pierce DA, Suyama A, Mabuchi K. Studies of mortality of atomic bomb survivors. Report 13: Solid cancer and noncancer disease mortality: 1950–1997. Radiat Res 2003;160:381–407.
37. Preston DL, Ron E, Tokuoka S, Funamoto S, Nishi N, Soda M, et al. Solid cancer incidence in atomic bomb survivors: 1958–1998 Radiat Res 2007;167:1–64.
38. Hall EJ, Brenner DJ. Cancer risks from diagnostic radiology. Br J Radiol 2008;81:362–78,
39. National Council on Radiation Protection and Measurements. Evaluation of the linear-non threshold dose-response model for ionizing radiation. Report No. 136. Bethesda, MD: NCRP, 2001.